# Associated production of Higgs and $Z$ bosons from gluon fusion in hadron collisions

Bernd A. Kniehl
*Department of Physics, University of Wisconsin, Madison, Wisconsin 53706*
(Received 19 April 1990)

Analytic results for the $ZHgg$ vertex are used to study the contribution of $pp \to ZH + X$ from gluon fusion, $gg \to ZH$, at supercollider energies. Because of the destructive interference between the triangle and the box amplitude, gluon fusion is suppressed as compared to quark-antiquark annihilation, $q\bar{q} \to ZH$, unless the masses of both the top quark and the Higgs boson assume values close to their theoretical upper bounds.

## I. INTRODUCTION

In the minimal standard model of electroweak interactions, the occurrence of a neutral Higgs boson $H$ is an inherent feature of the symmetry-breaking mechanism and its discovery would provide a crucial test of this theory. The vacuum expectation value of the Higgs particle is predicted to be equal to $2^{-1/4}G_F^{-1/2} \approx 246$ GeV, but its mass $M_H$ is only weakly constrained,[1] which renders it difficult to look for it. Recently, the experimental bound $M_H \geq 24$ GeV (Ref. 2) has been obtained at the CERN Large Electron Positron Collider (LEP). On the other hand, if $M_H$ exceeds 1 TeV, the Higgs boson becomes strongly coupled to the $W$ and $Z$ bosons and no longer behaves as a particle.[3]

One of the central objectives of future $pp$ colliders, such as the CERN Large Hadron Collider (LHC) and the Superconducting Super Collider (SSC), consists in searching for the Higgs boson in the heavy-mass region $M_H > 2M_W$. Above this threshold, the preferred decay modes are $H \to W^+W^-$, $H \to ZZ$, and $H \to t\bar{t}$. In hadron collisions, inclusive Higgs-boson production proceeds dominantly via gluon fusion,[4] $gg \to H$, which is mediated by quark triangle graphs, and $WW/ZZ$ fusion,[5] $qq \to qqH$, where the intermediate vector bosons are emitted from the initial quarks and annihilate to create a Higgs boson. Neutral-Higgs-boson production via $t\bar{t}$ fusion $gg \to t\bar{t}H$ has been comprehensively investigated in Refs. 6 and 7 and has been found generally smaller than the other two mechanisms.

Generally speaking, a hadron collider provides a less advantageous environment for detecting a Higgs boson than an $e^+e^-$ collider. Backgrounds to channels in which the Higgs boson decays to quark pairs, or to vector bosons which in turn decay to quark pairs, tend to obscure the signals. In order to reduce these backgrounds, it is inevitable to employ some kind of electromagnetic or leptonic trigger. In the production of a Higgs boson in conjunction with a $Z$ boson, the subsequent leptonic decay of the $Z$ boson would serve as a spectacular trigger for the Higgs-boson search. Associated $ZH$ production can already be realized on the tree level through quark-antiquark annihilation[8,9] $q\bar{q} \to ZH$. Because of the smallness of the heavy-quark structure functions, only the light quarks are relevant and in the massless quark approximation the Higgs boson is emitted from the $Z$-boson line [see Fig. 1(a)]. An alternative mechanism is provided by gluon fusion[10,11] $gg \to ZH$, which to lowest order proceeds through the triangle and box diagrams depicted in Fig. 1(b).

At first sight, one would expect the latter subprocess to be suppressed by the factor $(\alpha_s/\pi)^2$. This suppression is, however, partly compensated by the strong peaking of the gluon luminosity at small $\tau = \hat{s}/s$, where $\hat{s}$ denotes the invariant mass of the incoming partons. Furthermore, $\sigma(q\bar{q} \to ZH)$ drops rapidly for increasing $M_H$ due to the $s$-channel behavior of the $Z$-boson propagator. As a consequence of the Landau-Yang theorem,[12] this feature is absent in the triangle-type amplitude for $gg \to ZH$; the box graphs do not, of course, involve any virtual $Z$ bosons anyway. As has been observed in Ref. 10, the triangle contribution to $ZH$ production can, in fact, substantially exceed that from the usual light-quark sources, if the top quark is very heavy. *Ibidem* it has also been conjectured that, since the triangle diagram contributes to only one partial wave ($J = 0$) while the box diagram can contribute to all partial waves, the two graphs are essentially incoherent and that, consequently, the triangle graph gives a lower bound on the $gg \to ZH$ contribution.

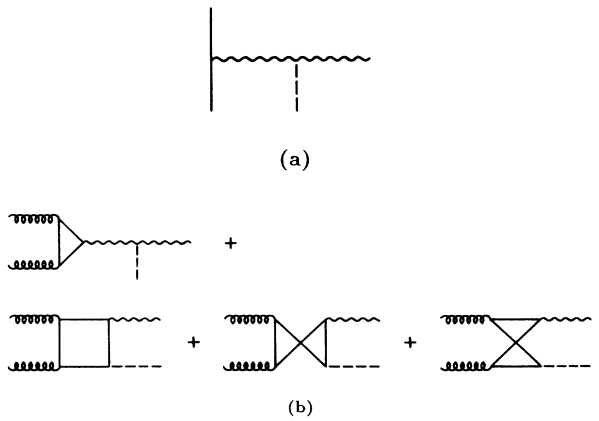


FIG. 1. Feynman diagrams pertinent to associated $ZH$ production via (a) quark-antiquark annihilation and (b) gluon fusion.

 

In this paper we calculate the full contribution from gluon fusion and show that the interference between the triangle and box amplitudes is mainly destructive. It turns out that quark-antiquark annihilation is the dominant parton level process for $ZH$ production, unless both $m_t$ and $M_H$ are settled in the very upper range of values currently preferred from theoretical arguments.

## II. PARTON CROSS SECTIONS

In a previous work[13] we have derived an analytic expression for the $ZHgg$ vertex to lowest order, which is generated by the set of diagrams depicted in Fig. 1(b). Thereby we have assumed that the vector bosons are real. In summary, we find for the $T$-matrix element of interest

$$i\mathcal{T}=\sqrt{2z}\,G_F\frac{\alpha_s}{\pi}\epsilon_\alpha^a(q_1)\epsilon_\beta^b(q_2)\epsilon_\mu(p)\delta^{ab}\times\sum_q I_q T^{\alpha\beta\mu}(q_1,q_2,p,m_q)\ , \tag{2.1}$$

where it is summed over the color indices $a,b=1,\ldots,8$, and the quark flavors $q$. $G_F$ is the Fermi constant, $\alpha_s$ is the strong coupling constant, and $I_q=\pm\frac{1}{2}$ is the third component of the weak isospin. $q_1$, $q_2$, $p$ are the four-momenta of the two gluons and the $Z$ boson, respectively, and $\epsilon^a(q_1)$, $\epsilon^b(q_2)$, $\epsilon(p)$ are their polarization four-vectors. We take all momenta to be ingoing and define

$$s=(q_1+q_2)^2,\quad t=(q_1+p)^2,\quad u=(q_2+p)^2\ ,$$

$$z=p^2,\quad h=(q_1+q_2+p)^2,\quad N=tu-zh\ .$$

The mass-shell conditions read $q_1^2=q_2^2=0$, $z=M_Z^2$, $h=M_H^2$. Momentum conservation leads to the identity $s+t+u=z+h$. The polarization tensor $T^{\alpha\beta\mu}(q_1,q_2,p,m)$ has the following decomposition:

$$\begin{aligned}T^{\alpha\beta\mu}(q_1,q_2,p,m)=&\left[\frac{s}{2}\epsilon^{\alpha\beta\mu\rho}q_{2\rho}-q_2^\alpha\epsilon^{\beta\mu\rho\sigma}q_{1\rho}q_{2\sigma}\right]F_1(t,u,z,h,m^2)-\left[\frac{s}{2}\epsilon^{\alpha\beta\mu\rho}q_{1\rho}-q_1^\beta\epsilon^{\alpha\mu\rho\sigma}q_{1\rho}q_{2\sigma}\right]F_1(u,t,z,h,m^2)\\&+\left[p^\alpha+\frac{z-t}{s}q_2^\alpha\right]\epsilon^{\beta\mu\rho\sigma}q_{2\rho}[q_{1\sigma}F_2(t,u,z,h,m^2)+p_\sigma F_3(t,u,z,h,m^2)]\\&+\left[p^\beta+\frac{z-u}{s}q_1^\beta\right]\epsilon^{\alpha\mu\rho\sigma}q_{1\rho}[q_{2\sigma}F_2(u,t,z,h,m^2)+p_\sigma F_3(u,t,z,h,m^2)]\\&+\left[\frac{s}{2}\epsilon^{\alpha\beta\mu\rho}p_\rho-q_2^\alpha\epsilon^{\beta\mu\rho\sigma}q_{1\rho}p_\sigma+q_1^\beta\epsilon^{\alpha\mu\rho\sigma}q_{2\rho}p_\sigma+g^{\alpha\beta}\epsilon^{\mu\rho\sigma\tau}q_{1\rho}q_{2\sigma}p_\tau\right]F_4(t,u,z,h,m^2)\ ,\end{aligned} \tag{2.2}$$

where we use the convention $\epsilon^{0123}=1$. Herein we have already dropped terms proportional to $q_1^\alpha$, $q_2^\beta$, or $p^\mu$ appealing to the transversality conditions for the vector bosons $q_1\cdot\epsilon^a(q_1)=q_2\cdot\epsilon^b(q_2)=p\cdot\epsilon(p)=0$. Applying the reduction algorithm developed in Ref. 14, the form factors $F_i(t,u,z,h,m^2)$ $(i=1,\ldots,4)$ can be expressed by means of three- and four-point functions $C_0$ and $D_0$, which on their part can be written in terms of complex logarithms and Spence functions.[15] The final result includes 136 Spence functions of distinct arguments and is listed in the Appendixes of Ref. 13. Gauge invariance and Bose symmetry with respect to the gluons are manifest

$$q_{1\alpha}T^{\alpha\beta\mu}(q_1,q_2,p,m)=q_{2\beta}T^{\alpha\beta\mu}(q_1,q_2,p,m)=0\ , \tag{2.3}$$

$$T^{\beta\alpha\mu}(q_2,q_1,p,m)=T^{\alpha\beta\mu}(q_1,q_2,p,m)\ . \tag{2.4}$$

As a consequence of charge conjugation invariance, the $Z$ boson couples only axially to the internal quark, so that the contribution from a mass-degenerate weak isodoublet of quarks vanishes. The dominant contribution is, therefore, expected to come from the $(t,b)$ doublet and the influence of the lighter quarks may safely be neglected.

As the bottom quark mass represents by far the smallest scale in the process, the corresponding scalar one-loop integrals may be well approximated by their small-$m^2$ expansions. They are presented in Appendix A of Ref. 13, except for $D_0(0,0,z,h,s,u,m^2)$. In the latter case, expanding in $m^2$ is straightforward with the exception of one set of Spence functions, in which subtle cancellations take place, viz.,

$$J\left[u,m^2,\frac{x_-}{\beta}\right]=\tfrac{1}{2}[\ln^2(u+i\epsilon)-\ln^2(-m^2+i\epsilon)]-\zeta(2)\ , \tag{2.5}$$

where we refer to the notation introduced in Ref. 13.

The $Z$ and the Higgs boson have opposite transverse momenta and $p_t^2=N/s$. The differential parton cross section is given by

$$\begin{aligned}&\frac{d\sigma(gg\to ZH)}{dp_t}=\frac{\sqrt{N}}{4\pi(u-t)s^{3/2}}\langle|\mathcal{T}|^2\rangle\ ,\\&0\le p_t\le\tfrac{1}{2}\sqrt{\lambda/s}\ ,\\&t=-\tfrac{1}{2}(s-z-h+\sqrt{\lambda-4sp_t^2})\ ,\\&u=z+h-s-t\ ,\end{aligned} \tag{2.6}$$

where

$$\lambda=\lambda(s,z,h)=s^2+z^2+h^2-2(sz+zh+hs)$$

and $\langle|\mathcal{T}|^2\rangle$ denotes the absolute squared of the invariant amplitude $\mathcal{T}$ after summing over the final polarizations and averaging over the initial ones and over color. The scalar coefficients which result from the contraction of the basic Lorentz tensors in Eq. (2.2) by pairs with the polarization tensors of the vector bosons are tabulated in the Appendix. Alternatively, the total cross section is most conveniently calculated as

$$\sigma(gg\to ZH)=\frac{1}{16\pi s^2}\times\int_{-(s-z-h+\sqrt{\lambda})/2}^{-(s-z-h-\sqrt{\lambda})/2}dt\,\langle|\mathcal{T}|^2\rangle_{u=z+h-s-t}\ . \quad (2.7)$$

For completeness, we also list the corresponding results for quark-antiquark annihilation

$$\frac{d\sigma(q\bar{q}\to ZH)}{dp_t}=\frac{G_F^2}{6\pi}(V_q^2+A_q^2)\frac{z^2}{(u-t)[(s-z)^2+z\Gamma_Z^2]}\times\sqrt{N/s}\left[z+\frac{N}{2s}\right], \quad (2.8)$$

$$\sigma(q\bar{q}\to ZH)=\frac{G_F^2}{24\pi}(V_q^2+A_q^2)\frac{z^2}{(s-z)^2+z\Gamma_Z^2}\frac{\sqrt{\lambda}}{s}\times\left[z+\frac{\lambda}{12s}\right]. \quad (2.9)$$

Here $V_q=2I_q-4\sin^2\theta_W Q_q$, $A_q=2I_q$, and $\theta_W$ denotes the weak mixing angle. In practical applications, the $Z$-boson width $\Gamma_Z$ may, of course, be neglected. Our expression for $\sigma(q\bar{q}\to ZH)$ agrees with the one derived in Ref. 9.

## III. DISCUSSION

In the numerical analysis we set $M_Z=91.15$ GeV, $\Gamma_Z=2.55$ GeV (Ref. 16), $\sin^2\theta_W=0.23$ (Ref. 17), $m_b=5$ GeV, and vary $m_t$ between 80 (Ref. 18) and 200 GeV (Ref. 19). We use set 1 of the parton distribution functions in Ref. 20, where $\Lambda_{\rm QCD}=200$ MeV is assumed for the asymptotic scale parameter. For the running QCD coupling constant $\alpha_s(Q^2)$ we employ the representation in the modified minimal-subtraction ($\overline{\rm MS}$) scheme of Eq. (6) in Ref. 21 with $\Lambda^{(6)}_{\overline{\rm MS}}=60$ MeV, which corresponds to $\Lambda^{(4)}_{\overline{\rm MS}}=200$ MeV for $m_t=100$ GeV, and we choose $Q^2=\hat{s}$ as renormalization scale. Since the mass splitting within the light-quark doublets $(u,d)$ and $(c,s)$ is insignificant as compared to the characteristic energy scale of the process, we neglect their contribution. We have checked that this amounts to an error of less than 0.5%, which has to be contrasted with the uncertainty introduced by the strong coupling constant $\delta\alpha_s^2/\alpha_s^2\approx 50\%$ due to the ambiguity in the choice of $Q^2$.

In view of crucial evidence for the number of light neutrino species being three,[22] we are not concerned with a fourth generation of quarks. However, in order to compare our calculation with the one in Ref. 11, we reconsider the cross section for $pp\to ZH+X$ from gluon fusion via a hypothetical quark doublet $(U,D)$, with $m_U=m_D+250$ GeV and $m_D=200$ GeV at the envisaged SSC energy $\sqrt{s}=40$ TeV, adopting all parameters specified there (see Fig. 2). Apart from an overall renormalization factor close to one, which is presumably attributed to our lack of knowledge of the precise parametrization of $\alpha_s$ and of the choice of the scale $Q^2$ used in that reference, we find agreement for the individual contributions from both the triangle (dashed line) and the set of box diagrams (dash-dotted line) but substantial disagreement as for their superposition (solid line). We are, however, able to reproduce the full prediction as of Fig. 3 of Ref. 11 when we multiply our box amplitude by an extra

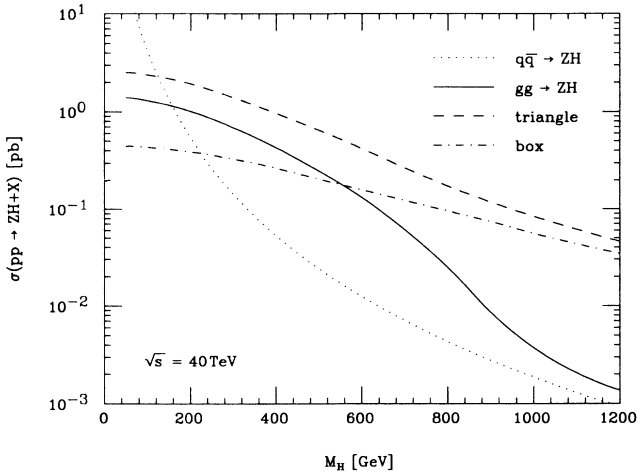


FIG. 2. Total cross section for $pp\to ZH+X$ from gluon fusion via a fourth generation of quarks with $m_U=m_D+250$ GeV and $m_D=200$ GeV (solid line) and quark-antiquark annihilation (dotted line) at $\sqrt{s}=40$ TeV. Also shown are the individual contributions from the triangle (dashed line) and the set of box diagrams (dash-dotted line).

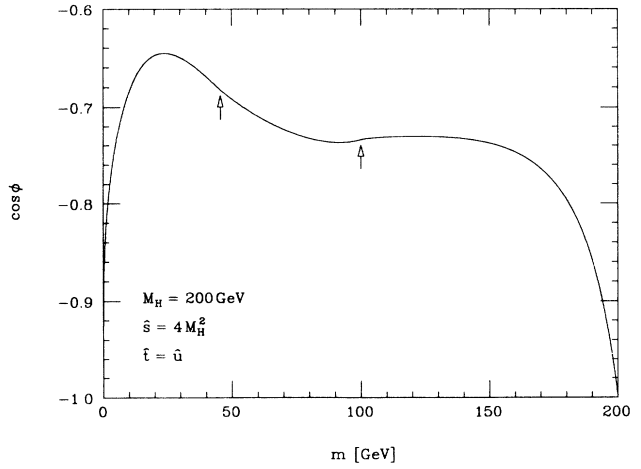


FIG. 3. Relative phase angle between the triangle and the box amplitude as a function of the mass of a single internal quark for a representative setting defined by $M_H=200$ GeV, $\hat{s}=4M_H^2$, and $\hat{t}=\hat{u}$. The arrows indicate the thresholds at $m=M_Z/2$ and $m=M_H/2$.

factor of $i$. This manipulation causes the result to increase by a factor of about 35 for $M_H = 1$ TeV. For comparison, also the contribution from quark-antiquark annihilation is shown (dotted line). Note that, in contrast to quark-antiquark annihilation, gluon fusion yields the same contribution in proton-antiproton collisions.

From Fig. 2 it is apparent that the triangle-box interference is, for the most part, destructive. This can be worked out already on the basis of squared matrix elements. To that end, we define the relative phase angle $\phi$ between the triangle and the box amplitude $\mathcal{T}_T$ and $\mathcal{T}_B$ by

$$\langle|\mathcal{T}_T+\mathcal{T}_B|^2\rangle=\langle|\mathcal{T}_T|^2\rangle+\langle|\mathcal{T}_B|^2\rangle +2(\langle|\mathcal{T}_T|^2\rangle\langle|\mathcal{T}_B|^2\rangle)^{1/2}\cos\phi\ . \quad (3.1)$$

Figure 3 displays the variation of $\cos\phi$ with the mass $m$ of a single internal quark assuming an exemplary situation where $\hat{s}=4M_H^2$ with $M_H=200$ GeV and where the $Z$ and the Higgs boson are emitted perpendicularly to the gluons in the center-of-mass system. Figuratively speaking, $\mathcal{T}_T$ and $\mathcal{T}_B$ point in two directions in the complex plane which are opposite within a tolerance of less than 50°. The two inflection points at $m=M_Z/2$ and $m=M_H/2$ (see arrows) are due to imaginary parts in $\mathcal{T}_B$ which are switched off as the internal quark becomes too heavy to be pair-produced through $Z$- and Higgs-boson decay, respectively. Eventually, above the threshold $m=\sqrt{\hat{s}}/2$ both $\mathcal{T}_T$ and $\mathcal{T}_B$ are real and opposite in sign. In fact, as has already been mentioned in Ref. 13, the leading terms in the large-$m^2$ expansions of $\mathcal{T}_T$ and $\mathcal{T}_B$ are both proportional to $1/m^2$ but, apart from finite-width effects, they cancel each other leaving behind terms of $O(1/m^4)$.

Figure 4 shows the transverse momentum distributions for $pp\to ZH+X$ at $\sqrt{s}=40$ TeV arising from gluon fusion (solid lines) and quark-antiquark annihilation (dotted lines) for $m_t=80$, 140, 200 GeV and $M_H=30$, 100, 500 GeV. They are all finite in the limit $p_t\to 0$. Taking into account the triangle diagram along (dashed line) greatly overestimates the contribution from $gg\to ZH$ throughout, especially for large $p_t$. While $q\bar{q}\to ZH$ is insensitive to $m_t$, as has been explained in the Introduction, $gg\to ZH$ attains relative importance as $m_t$ increases. The channel $q\bar{q}\to ZH$ is, however, clearly dominant in the high-$p_t$ range, $p_t>400$ GeV, independently of $M_H$. The only chance for gluon fusion to be competitive is in the window 200 GeV $<p_t<$ 400 GeV if $m_t$ is close to 200 GeV and $M_H<300$ GeV. The spikes in the $p_t$ spectra from $gg\to ZH$ may be understood as genuine threshold effects and they are located at

$$p_t=\frac{[\lambda(4m_t^2,M_Z^2,M_H^2)]^{1/2}}{4m_t}\ , \quad (3.2)$$

where $\hat{s}$ is sufficiently large to create toponium provided that no energy is used up for longitudinal motion in the $ZH$ system. These serrations disappear for $2m_t\le M_Z+M_H$, when toponium can already mix with $ZH$ produced at rest.

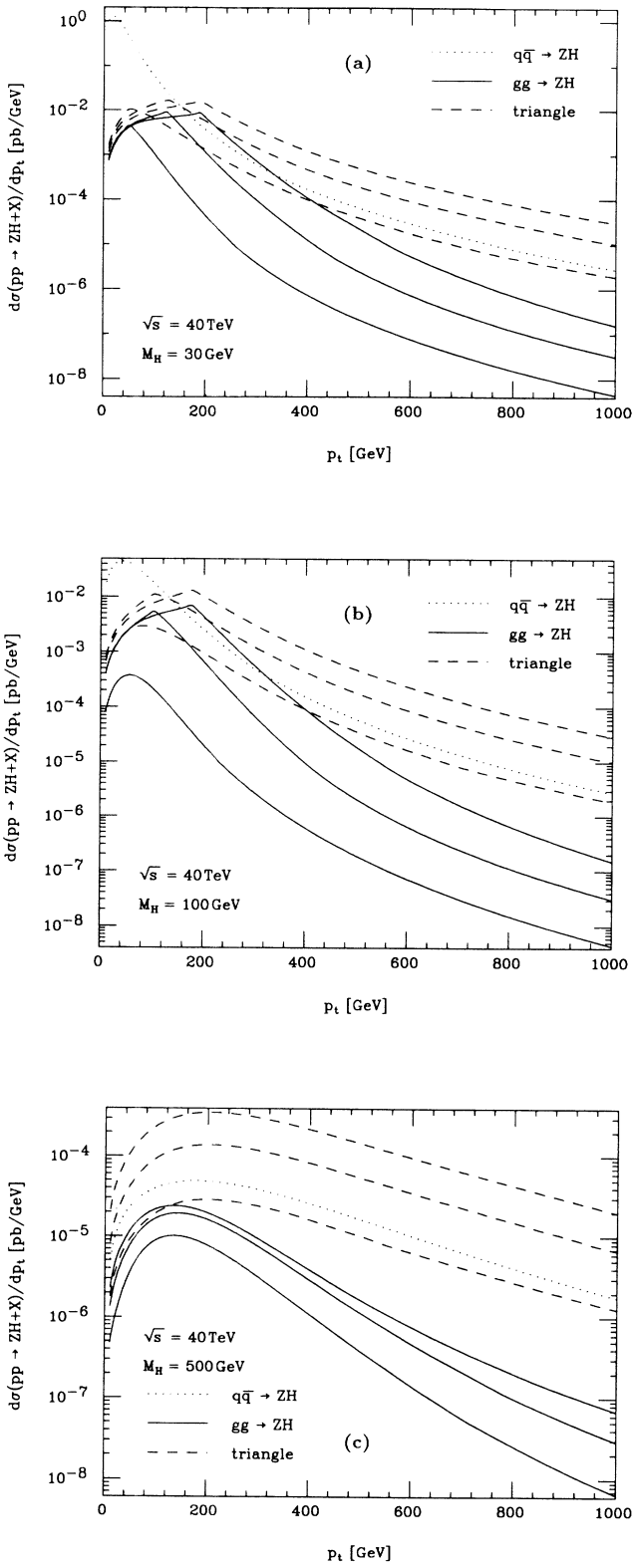


FIG. 4. Transverse-momentum distributions for $pp\to ZH+X$ at $\sqrt{s}=40$ TeV from gluon fusion for $m_t=80$, 140, 200 GeV (solid lines) and from quark-antiquark annihilation (dotted lines) for (a) $M_H=30$ GeV, (b) $M_H=100$ GeV, and (c) $M_H=500$ GeV. Lower curves correspond to smaller values of $m_t$.

Figure 5 visualizes the $M_H$ dependence of the total cross section for $pp \to ZH + X$ from gluon fusion choosing $m_t = 80$, 140, 200 GeV (solid lines) and from quark-antiquark annihilation (dotted lines) at the LHC and SSC energies, $\sqrt{s} = 17$ and 40 TeV. The triangle contribution by itself (dashed lines) leads to a poor description as to both size and line shape. The full contribution from $gg \to ZH$ drops rapidly for increasing $M_H$ until it enters a plateau at the threshold $M_H = 2m_t$. It is interesting to recall that also $\sigma(pp \to H + X)$ via $gg \to H$, which is plotted as a function of $M_H$ in Fig. 1 of Ref. 7, exhibits a striking dent at about $M_H = 2m_t$ for $m_t = 200$ GeV. This suggests to interpret the emission of the additional $Z$ boson in $gg \to ZH$ as some kind of bremsstrahlung correction for $gg \to H$ assuming that $M_Z \ll M_H, m_t$. As has been anticipated in the Introduction, the support from gluon fusion surpasses that from quark-antiquark annihilation only for $m_t \lesssim 200$ GeV and $M_H \lesssim 1$ TeV. One should, however, keep in mind that our analysis does not include subsequent decays of the Higgs boson and is, therefore, of limited predicatory power for large $M_H$. Should the top quark be very heavy, the channels $q\bar{q} \to ZH$ and $gg \to ZH$ are comparable sources of Higgs bosons in the window $200\ \text{GeV} < M_H < 300\ \text{GeV}$ at the SSC.

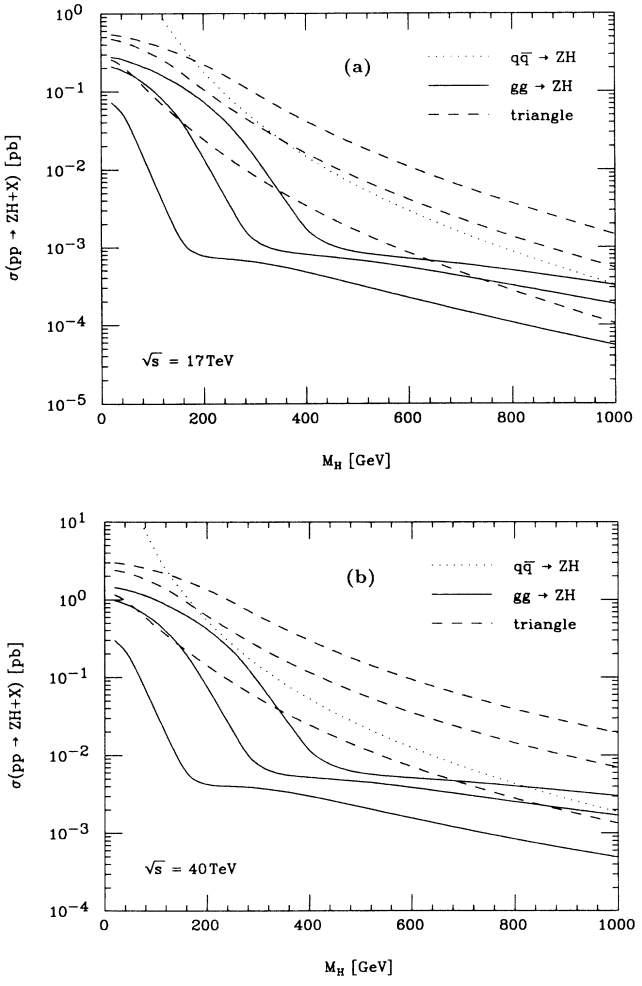


FIG. 5. Total cross section for $pp \to ZH + X$ from gluon fusion for $m_t = 80$, 140, 200 GeV (solid lines) and from quark-antiquark annihilation (dotted lines) at (a) $\sqrt{s} = 17$ TeV and (b) $\sqrt{s} = 40$ TeV. Lower curves correspond to smaller values of $m_t$.

## IV. CONCLUSIONS

Using an analytic expression for the $ZHgg$ vertex derived previously, we have calculated the parton cross section for the subprocess $gg \to ZH$ within the minimal standard model (three fermion generations, one neutral Higgs boson) and investigated the contribution from this channel to associated $ZH$ production at supercollider energies. We find that gluon fusion is in competition with the three-level process $q\bar{q} \to ZH$ as for Higgs-boson searches in the window $200 < M_H < 300$ GeV at the SSC provided the top quark is sufficiently heavy. If the Higgs boson is looked for via its decay mode $H \to ZZ$ (branching ratio $B \approx \frac{1}{3}$) with subsequent decays of the $Z$ bosons in electrons or muons ($B \approx 6.8\%$), then $\sigma(pp \to ZH + X) = 1$ pb corresponds to a yield of 15 events per one year of running at the SSC assuming an integrated luminosity of $10^4$ pb$^{-1}$.[23] If the primary $Z$ boson is identified through its decay into pairs of electrons, muons, or neutrinos ($B \approx 27.3\%$), the annual number of these events is reduced to four, the detection of which could just be at the edge of manageable goals.

## ACKNOWLEDGMENTS

We would like to acknowledge beneficial discussions with U. Baur and E. Zas. This research was supported in part by the University of Wisconsin Research Committee with funds granted by the Wisconsin Alumni Research Foundation, and in part by the U.S. Department of Energy under Contract No. DE-AC02-76ER00881.

## APPENDIX

In the computation of $\langle |\mathcal{T}|^2 \rangle$ one encounters Lorentz scalars of the form

$$c_{ij} = c_{ji} = -g_{\alpha\gamma} g_{\beta\delta} \left[ g_{\mu\nu} - \frac{p_\mu p_\nu}{z} \right] \times T_i^{\alpha\beta\mu}(q_1, q_2, p) T_j^{\gamma\delta\nu}(q_1, q_2, p) , \quad i,j = 1, \ldots, 7 , \tag{A1}$$

where

$$T_1^{\alpha\beta\mu}(q_1, q_2, p) = T_2^{\beta\alpha\mu}(q_2, q_1, p) = \frac{s}{2} \epsilon^{\alpha\beta\mu\rho} q_{2\rho} - q_2^\alpha \epsilon^{\beta\mu\rho\sigma} q_{1\rho} q_{2\sigma} ,$$

$$T_3^{\alpha\beta\mu}(q_1, q_2, p) = T_4^{\beta\alpha\mu}(q_2, q_1, p) = \left[ p^\alpha + \frac{z - t}{s} q_2^\alpha \right] \epsilon^{\beta\mu\rho\sigma} q_{2\rho} q_{1\sigma} , \tag{A2}$$

$$T_5^{\alpha\beta\mu}(q_1,q_2,p)=T_6^{\beta\alpha\mu}(q_2,q_1,p)$$
$$=\left[p^\alpha+\frac{z-t}{s}q_2^\alpha\right]\epsilon^{\beta\mu\rho\sigma}q_{2\rho}p_\sigma\ ,$$
$$T_7^{\alpha\beta\mu}(q_1,q_2,p)=\frac{s}{2}\epsilon^{\alpha\beta\mu\rho}p_\rho-q_2^\alpha\epsilon^{\beta\mu\rho\sigma}q_{1\rho}p_\sigma$$
$$+q_1^\beta\epsilon^{\alpha\mu\rho\sigma}q_{2\rho}p_\sigma$$
$$+g^{\alpha\beta}\epsilon^{\mu\rho\sigma\tau}q_{1\rho}q_{2\sigma}p_\tau\ .$$

For the reader's convenience, we list these coefficients below:

$$c_{11}=\frac{s^2(z-u)^2}{8z},\quad c_{12}=\frac{s^2}{8}\left[\frac{N}{z}-s\right],$$
$$c_{13}=c_{14}=\frac{sN}{8}\left[1-\frac{u}{z}\right],\quad c_{15}=c_{26}=0\ ,$$
$$c_{16}=c_{25}=c_{34}=-c_{37}=c_{47}=-\frac{sN}{4}\ ,$$
$$c_{17}=\frac{s^2}{4}(u-z),\quad c_{22}=\frac{s^2(z-t)^2}{8z}\ ,$$
$$c_{23}=c_{24}=\frac{sN}{8}\left[1-\frac{t}{z}\right],\quad c_{27}=\frac{s^2}{4}(z-t)\ ,$$
$$c_{33}=c_{44}=\frac{N}{2}\left[s+\frac{N}{2z}\right],$$
$$c_{35}=-2c_{45}=c_{57}=\frac{N}{2}(u-z)\ ,$$
$$c_{46}=-2c_{36}=-c_{67}=\frac{N}{2}(t-z)\ ,$$
$$c_{55}=\frac{N}{2s}(z-u)^2,\quad c_{56}=-\frac{N}{4}\left[z+\frac{N}{s}\right],$$
$$c_{66}=\frac{N}{2s}(z-t)^2,\quad c_{77}=s\left[N+\frac{sz}{2}\right].$$

(A3)


[1]S. Coleman and E. Weinberg, Phys. Rev. D 7, 1888 (1973).

[2]ALEPH Collaboration, Z. Ajaltouni *et al.*, Phys. Lett. B **236**, 233 (1990); **241**, 141 (1990).

[3]D. A. Dicus and V. S. Mathur, Phys. Rev. D 7, 3111 (1973); M. Veltman, Acta Phys. Pol. B **8**, 475 (1977); B. W. Lee, C. Quigg, and H. B. Thacker, Phys. Rev. Lett. **38**, 883 (1977); Phys. Rev. D **16**, 1519 (1977).

[4]H. M. Georgi, S. L. Glashow, M. E. Machacek, and D. V. Nanopoulos, Phys. Rev. Lett. **40**, 692 (1978).

[5]R. N. Cahn and S. Dawson, Phys. Lett. **136B**, 196 (1984); **138B**, 464(E) (1984); S. Dawson, Nucl. Phys. **B249**, 42 (1984).

[6]Z. Kunszt, Nucl. Phys. **B247**, 339 (1984).

[7]J. F. Gunion, H. E. Haber, F. E. Paige, W.-K. Tung, and S. S. D. Willenbrock, Nucl. Phys. **B294**, 621 (1987).

[8]S. L. Glashow, D. V. Nanopoulos, and A. Yildiz, Phys. Rev. D **18**, 1724 (1978).

[9]E. Eichten, I. Hinchliffe, K. Lane, and C. Quigg, Rev. Mod. Phys. **56**, 579 (1984); **58**, 1065(E) (1986).

[10]V. Barger, E. W. N. Glover, K. Hikasa, W.-Y. Keung, M. G. Olsson, C. J. Suchyta, and X. R. Tata, Phys. Rev. Lett. **57**, 1672 (1986).

[11]D. A. Dicus and C. Kao, Phys. Rev. D **38**, 1008 (1988).

[12]L. D. Landau, Dok. Akad. Nauk SSSR **60**, 207 (1948); C. N. Yang, Phys. Rev. **77**, 242 (1949).

[13]B. A. Kniehl, Phys. Rev. D (to be published).

[14]G. 't Hooft and M. Veltman, Nucl. Phys. **B153**, 365 (1979); G. Passarino and M. Veltman, *ibid.* **B160**, 151 (1979).

[15]R. Lewin, *Dilogarithms and Associated Functions* (MacMillan, London, 1958).

[16]J. Thresher, presented at the Annual Meeting of the Division of Particles and Fields of the APS, Houston, Texas, 1990 (unpublished).

[17]Particle Data Group, G. P. Yost *et al.*, Phys. Lett. B **204**, 1 (1988).

[18]CDF Collaboration, F. Abe *et al.*, Phys. Rev. Lett. **64**, 142 (1990).

[19]P. Langacker, Phys. Rev. Lett. **63**, 1920 (1989).

[20]D. W. Duke and J. F. Owens, Phys. Rev. D **30**, 49 (1984).

[21]W. J. Marciano, Phys. Rev. D **29**, 580 (1984).

[22]OPAL Collaboration, M. Z. Akrawy *et al.*, Phys. Lett. B **231**, 530 (1989); DELPHI Collaboration, P. Aarnio *et al.*, *ibid.* **231**, 539 (1989); ALEPH Collaboration, Z. Ajaltouni *et al.*, *ibid.* **235**, 399 (1990); L3 Collaboration, B. Adeva *et al.*, *ibid.* **237**, 136 (1990).

[23]R. N. Cahn *et al.*, in *Experiments, Detectors, and Experimental Areas for the Supercollider,* proceedings of the Workshop, Berkeley, California, edited by R. Donaldson and M. G. D. Gilchriese (World Scientific, Singapore, 1988), p. 20.